EXPERIMENTAL DETECTION OF THE CNO CYCLE*

M. Misiaszek

on behalf of the Borexino Collaboration†

M. Smoluchowski Institute of Physics, Jagiellonian University
30-348 Kraków, Poland

Received 22 April 2022, accepted 10 May 2022,
published online 9 September 2022

Borexino recently reported the first experimental evidence for a CNO neutrino. Since this process accounts for only about 1% of the Sun's total energy production, the associated neutrino flux is remarkably low compared to that of the *pp* chain, the dominant hydrogen-burning process. This experimental evidence for the existence of CNO neutrinos was obtained using a highly radio-pure Borexino liquid scintillator. Improvements in the thermal stabilization of the detector over the last five years have allowed us to exploit a method of constraining the rate of ^{210}Bi background. Since the CNO cycle is dominant in massive stars, this result is the first experimental evidence of a major stellar hydrogen-to-helium conversion mechanism in the Universe.

DOI:10.5506/APhysPolBSupp.15.3-A24

1. Introduction

Stars are fueled by a nuclear fusion of light elements with the release of an enormous amount of energy. In particular, the *pp* chain and the CNO cycle, also active in the Sun, produce a rich spectrum of electron-flavor neutrinos detectable on Earth [1, 2]. Those two mechanisms basically convert four hydrogen nuclei into a helium nucleus: the first uses a direct process throughout a wide variety of branches, while the second uses a closed-loop starting and ending with ^{12}C acting as a catalyst.

The contribution of these two mechanisms in the energy production is related to the mass, and then to the core temperature of the stars and to the abundance of elements heavier than helium in the core (in the jargon, "metallicity").

* Presented at the 28$^{\text{th}}$ Cracow Epiphany Conference on *Recent Advances in Astroparticle Physics*, Cracow, Poland, 10–14 January, 2022.

† The list of Borexino Collaboration members can be found at the end of the article.

For stars heavier than $1.3\,M_{\odot}$, the CNO cycle is the dominant process of hydrogen fusion [3], while in the Sun, with a core temperature of about 15×10^6 K, the CNO accounts only for 1% of the total luminosity, with a large uncertainty related to poorly-known metallicity [4]. The Borexino experiment, from mid-2007, has published a comprehensive study of neutrinos from the *pp* chain [5] and has recently reported the first direct detection of CNO [6]. The quest for CNO started by Borexino could, in principle, create a situation that makes possible the solution of the long-standing "solar metallicity problem" [2], *i.e.* the disagreement between the metallicity predicted by solar models using updated (low) metal abundances from spectroscopy (SSM-LZ) [7] and the one obtained from helioseismology, which predicts a higher metal content (SSM-HZ).

2. The Borexino detector

The Borexino experiment is the only experiment capable to detect solar neutrinos with a threshold as low as about 150 keV, and to reconstruct the position and the energy of each event in real time.

Borexino is located in the Hall C of Laboratori Nazionali Gran Sasso (INFN) [8]. The detector is made of concentric shells with increasing radiopurity (see *e.g.* Ref. [9]): the innermost core, enclosed in an ultrapure 125 μm thick nylon vessel of radius 4.25 m, is made of 300 tons of liquid scintillator (1,2,4-trimethylbenzene with 1.5 g/l of PPO wavelength shifter). The active core is contained by a stainless steel sphere filled with $\sim$ 1000 buffer liquid (1,2,4-trimethylbenzene with DMP quencher), whose internal surface is instrumented with more than 2000 PMTs to detect scintillation light. Finally, the SSS is located inside a 2000 ton water Cherenkov detector, equipped with about 200 PMTs. The Borexino detector is capable of reconstructing the position of the event with an accuracy of $\sim$ 10 (at 1 MeV) and an energy resolution of approximately $\sigma(E)/E = 5\%/\sqrt{(E/[\mathrm{MeV}])}$.

Due to its unprecedented radio-purity, Borexino has also set a lot of limits on rare processes (see *e.g.* [10–14]) and performed other neutrino physics studies, *e.g.* geo-neutrino detection (for review, see *e.g.* [15]). The CNO detection has required, as is explained in Section 3, an independent constraint of the ^{210}Bi contaminant from the ^{210}Po through the secular equilibrium. Figure 1 shows the ^{210}Po contaminant evolution during the thermal insulation program in 59 small cubes enumerated from bottom to top within a radius of 3 m from the center of the Inner Vessel. The red (black) superimposed curve represents the average temperature in the same region. The dashed vertical lines show the most important milestones of the temperature stabilization program: 1. Beginning of insulation; 2. Turning off the water recirculation system in the Water Tank; 3. The first operation of the active

temperature control system; 4. Change of the active control setpoint; 5. Installation and commissioning of the Hall C temperature control system. The white vertical bands represent different technical DAQ breaks. The ^{210}Po shown in the figure is a tracker of convective movements that are drastically damped as a consequence of the insulation program.

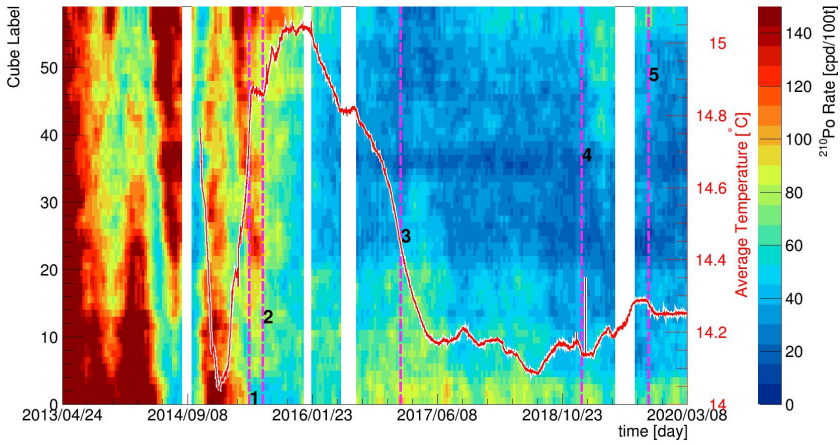

Fig. 1. (Color online) Evolution of the ^{210}Po contamination during the thermal insulation program.

3. CNO detection strategy

Neutrinos emitted in the CNO cycle have a continuous spectrum with a maximum energy of 1.74 MeV (see Fig. 2, left). In addition to the low rate, the main difficulty in detecting CNO neutrinos with Borexino is the presence of two radioactive backgrounds that produce signals in approximately the same energy region: ^{11}C and ^{210}Bi. Furthermore, solar neutrinos also from the *pep* reaction are a significant background for the CNO analysis. Figure 2 (right) shows a Monte Carlo simulation of the energy spectrum of electrons scattered by neutrinos from the CNO cycle (red line) compared to the signal induced by the radioactive decay of ^{11}C (purple line) and ^{210}Bi (green line). The blue line is the *pep* signal. The relative proportion of the four contributions is approximately the one expected in reality.

Cosmogenic ^{11}C is an isotope produced by residual muons that cross the scintillator, which decays and emits a positron with a lifetime of approximately 30 min. It can be tagged using the three-fold coincidence (TFC) method described in [16]. Separating the CNO signal from the ^{210}Bi and *pep* signal is more tricky since their spectral shapes are quite similar and the multivariate fit has a trouble with distinguishing between them, if no additional external constraints are imposed. For *pep* neutrinos, we exploited

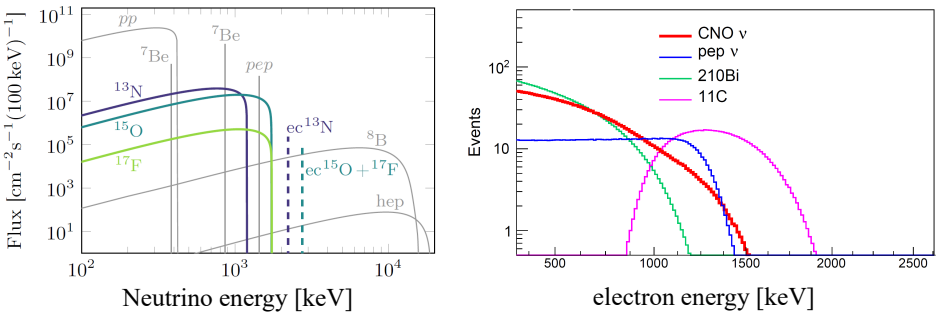

Fig. 2. (Color online) (left): Energy spectrum of neutrinos emitted in the CNO cycle (colored lines); (right): energy spectrum in Borexino for events of CNO (red), *pep* (blue), ^{210}Bi (green), and ^{11}C (purple) obtained from Monte Carlo simulations.

the external and independent information coming from the available solar neutrino data, solar luminosity, and the most recent oscillation parameters to put a constraint on their rate in fit with a 1.4% uncertainty. The remaining obstacle to the detection of CNO neutrinos is the contamination of ^{210}Bi. If secular equilibrium holds, the activities of ^{210}Bi and ^{210}Po are the same. Measuring the ^{210}Po rate is in principle, straightforward since alpha/beta discrimination techniques provide a powerful additional tool to isolate the ^{210}Po events.

Based on these premises, our strategy for the CNO detection relies on the ^{210}Bi–^{210}Po link to determine independently the ^{210}Bi content from ^{210}Po and constrain it in multivariate fit.

4. The ^{210}Bi–^{210}Po link

In order to exploit the ^{210}Bi–^{210}Po link to obtain an external constraint on the ^{210}Bi rate, we carefully studied the evolution in time and the spatial distribution of the polonium contamination in the detector during Borexino data collection. The ^{210}Po present in the fiducial region used in the analysis (an innermost subset of the volume of the scintillator) is actually the sum of two contributions: ^{210}Po from the intrinsic ^{210}Pb scintillator contamination (in equilibrium with ^{210}Bi); ^{210}Po from the nylon vessel containing the scintillator. This last contribution was found to change over time and was highly correlated with variations of the temperature gradient in the detector, which induce convective motions strong enough to bring ^{210}Po from the vessel surface into the fiducial region. To reduce these convective motions, we thermally insulated the detector, as discussed in Section 2.

After completion of thermal insulation (2016), the detector temperature has become very stable and the convective currents inside the scintillator have been significantly reduced. This has favored the formation of an innermost region of the detector, called the Low Polonium Field (LPoF), where the contribution to the ^{210}Po rate coming from the vessel is very small. The qualitative shape and approximate position of the LPoF is reproduced by fluid dynamical numerical simulations reported in [17].

From the 3D fit, we extract the ^{210}Po minimum. This value may still have a small contribution of ^{210}Po from the vessel component; therefore, this method provides only an upper limit for the ^{210}Bi rate. To cross-check the results, we performed the fit in different ways: adopting a standard likelihood fit with ROOT or a Bayesian tool called MultiNest. In addition to the 2D paraboloidal fit, we also performed the fit with a 3D ellipsoidal function or, alternatively, with a cubic spline. Differences in results were included in the systematic error associated with the upper limit on ^{210}Bi.

In the analysis to extract the neutrino rate of the CNO, which will be described in Section 5, we need to verify that ^{210}Bi is uniform in this volume during the time period over which the estimate is performed. For this reason, we studied the spatial distribution of β-like events in an energy window where the bismuth contribution is maximized. This distribution was found to be uniform within errors.

The final upper limit on ^{210}Bi including statistical and systematical errors added in quadrature is

$$\text{Rate}\left(^{210}\text{Bi}\right) \leq (11.5 \pm 1.3) \text{ cpd/100 t}\,.$$

5. Spectral analysis

We performed a multivariate analysis, simultaneously fitting the energy spectra in the window between 320 and 2640 keV and the radial distribution of the selected events, using data collected from June 2016 to February 2020 (Borexino Phase-III). The fiducial volume (FV) is defined as $r < 2.8$ m and z in the interval $(-1.8$ m, 2.2 m) (r and z are the reconstructed radial and vertical positions, respectively). The total exposure corresponds to 1072 days $\times 71.3$ t. The free parameters in the fit procedure are: the interaction rate of CNO neutrinos, ^{85}Kr, ^{11}C, internal and external ^{40}K, external ^{208}Tl and ^{214}Bi, and ^{7}Be neutrinos. The *pep* neutrino rate is constrained to to 2.74 ± 0.04 cpd per 100 t by multiplying the standard likelihood with a symmetric Gaussian term. The upper limit to the ^{210}Bi rate is the one reported in the previous section. It is enforced asymmetrically by multiplying the likelihood by a half-Gaussian term, that is, leaving the ^{214}Bi rate unconstrained between 0 and 11.5 cpd per 100 t.

The reference spectral and radial distributions of each signal and background species are obtained with a complete Monte Carlo simulation, which models all physics processes occurring in the scintillator. The results of the simultaneous multivariate fit of the energy spectra are given in Fig. 3, showing the TFC-subtracted and TFC-tagged data. The fit clearly prefers a nonzero CNO neutrino rate, as also shown in a detailed study of the log-likelihood profile.

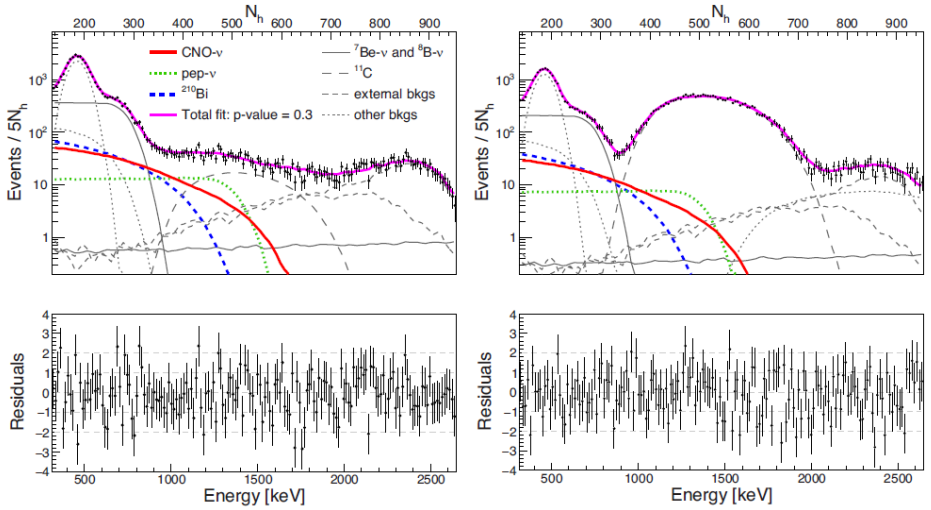

Fig. 3. (Color online) Energy distributions from a multivariate fit of the Borexino data. Full multivariate fit results for the TFC-subtracted (left) and the TFC-tagged (right) energy spectra with corresponding residuals. In both graphs, the magenta (the first from the top) lines represent the resulting fit function, the red solid line is the CNO neutrino electron recoil spectrum, the green dotted line is the *pep* neutrino electron recoil spectrum, the dashed blue line is the $^{210}\beta$ spectrum, and in grey we report the remaining background (bkgs) contributions.

The best fit value of the CNO neutrinos interaction rate is 7.2 cpd per 100 t with an asymmetric confidence interval of -1.7 cpd per 100 t and $+2.9$ cpd per 100 t (68% C.L.), considering only the statistical error. The many details of the analysis, including the list and evaluation of systematic effects, are reported in [6]. Folding the systematic uncertainty over the log-likelihood profile (Fig. 4), we determine that the final CNO interaction rate is $7.2^{+3}_{-1.7}$ cpd per 100 t. The rate can be converted to CNO neutrinos on Earth of $7.2^{+3.0}_{-2.0} \times 10^8$ cm^{-2} s^{-1} assuming MSW conversion in matter and the density of electrons in the scintillator of $(3.307 \pm 0.015) \times 10^{31}$ e^- per 100 t.

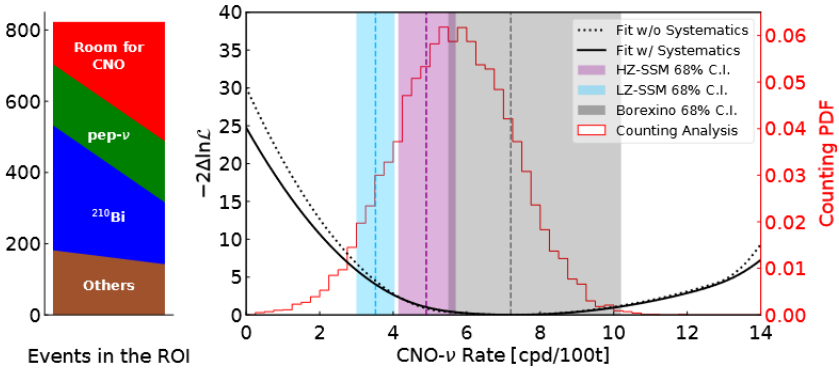

Fig. 4. (Color online) Results of the CNO counting and spectral analyses. Left: Counting analysis bar chart. The height represents the number of events allowed by the data for CNO neutrinos and backgrounds in the ROI; on the left, the CNO signal is minimum and backgrounds are maximum, while on the right, CNO is maximum and backgrounds are minimum. It is clear from this figure that CNO cannot be zero. Right: CNO neutrinos rate negative log-likelihood profile directly from the multivariate fit (dashed black line) and after folding in the systematic uncertainties (black solid line). Histogram in red: CNO neutrino rate obtained from the counting analysis. Finally, the blue, violet, and grey vertical bands (from left to right, respectively) show 68% confidence intervals (C.I.) for the SSM-LZ (3.52 ± 0.52 cpd per 100 t) and SSM-HZ (4.92 ± 0.78 cpd per 100 t) predictions and the Borexino result (corresponding to black solid line log-likelihood profile), respectively.

To evaluate the significance of our result in rejecting the hypothesis without CNO, we performed a frequentist hypothesis test using the profile likelihood that allows us to reject the CNO = 0 hypothesis with a significance better than 5.0σ at 99.0% C.L. The results of the analysis based on the fit are also confirmed by that obtained with a nearly independent method (counting analysis), in which we simply count events in an optimized energy window (region of interest, ROI) and subtract the contributions due to known backgrounds. This method reveals a non-zero CNO signal and its consistency with the multivariate analysis is remarkable. This method is simpler, albeit less powerful, with respect to the multivariate fit and is less prone to possible correlations between different species.

6. Conclusions

We have reported the results of the first direct detection of neutrinos from the CNO cycle in the Sun. This result proves the existence of the primary mechanism for the stellar conversion of hydrogen to helium in the

Universe. The observation of CNO neutrinos experimentally confirms the overall solar picture and shows that a direct measurement of the metallicity of the Sun's core is within the reach of improved future measurement.

We presented the results of the first direct neutrino detection from the CNO cycle in the Sun. This result proves the existence of the primary mechanism for the stellar conversion of hydrogen to helium in the Universe. Observation of CNO neutrinos experimentally confirms the Standard Model of the Sun and shows that the direct measurement of solar core metallicity is in the range of improved future measurements.

The authors acknowledge the generous hospitality and support of the Laboratori Nazionali del Gran Sasso (Italy). The Borexino program is made possible by funding from Istituto Nazionale di Fisica Nucleare (INFN) (Italy), the National Science Foundation (NSF) (USA), Deutsche Forschungsgemeinschaft (DFG) and Helmholtz-Gemeinschaft (HGF) (Germany), the Russian Foundation for Basic Research (RFBR) (grants No. 16-29-13014 ofi-m, No. 17-02-00305A, and No. 19-02-00097A), the Russian Science Foundation (RSF) (grant No. 17-12-01009) (Russia), and National Science Centre (NCN), Poland (grant No. UMO 2017/26/M/ST2/00915) (Poland). We gratefully acknowledge the computing services of Bologna INFN-CNAF data center and the U-Lite Computing Center and Network Service at LNGS (Italy), and the computing time granted through JARA on the JURECA supercomputer at the Forschungszentrum Jülich (Germany). This research was supported in part by PLGrid Infrastructure (Poland).

REFERENCES

[1] J.N. Bahcall, «Neutrino Astrophysics», *Cambridge University Press*, 1989.

[2] N. Vinyoles *et al.*, «A New Generation of Standard Solar Models», *Astrophys. J.* **835**, 202 (2017).

[3] M. Salaris, S. Cassisi, «Evolution of Stars and Stellar Populations», *John Wiley & Sons, Ltd*, Chichester, UK 2006.

[4] C. Angulo *et al.*, «A compilation of charged-particle induced thermonuclear reaction rates», *Nucl. Phys. A* **656**, 3 (1999).

[5] M. Agostini *et al.*, «Comprehensive measurement of *pp*-chain solar neutrinos», *Nature* **562**, 505 (2018).

[6] The Borexino Collaboration, «Experimental evidence of neutrinos produced in the CNO fusion cycle in the Sun», *Nature* **587**, 577 (2020).

[7] A.M. Serenelli, W. C. Haxton, C. Peña-Garay, «Solar Models with Accretion. I. Application to the Solar Abundance Problem», *Astrophys. J.* **743**, 24 (2011).

[8] Website: https://www.lngs.infn.it

[9] G. Alimonti *et al.*, «Science and technology of Borexino: a real-time detector for low energy solar neutrinos», *Astropart. Phys.* **16**, 205 (2002).

[10] A. Vishneva *et al.*, «Test of the electron stability with the Borexino detector», *J. Phys.: Conf. Ser.* **888**, 012193 (2017).

[11] S.K. Agarwalla *et al.*, «Constraints on flavor-diagonal non-standard neutrino interactions from Borexino Phase-II», *J. High Energy Phys.* **2002**, 038 (2020).

[12] M. Agostini *et al.*, «Search for low-energy neutrinos from astrophysical sources with Borexino», *Astropart. Phys.* **125**, 102509 (2021).

[13] M. Agostini *et al.*, «Limiting neutrino magnetic moments with Borexino Phase-II solar neutrino data», *Phys. Rev. D* **96**, 091103 (2017).

[14] G. Bellini *et al.*, «New limits on heavy sterile neutrino mixing in decay obtained with the Borexino detector», *Phys. Rev. D* **88**, 072010 (2013).

[15] M. Agostini *et al.*, «Comprehensive geoneutrino analysis with Borexino», *Phys. Rev. D* **101**, 012009 (2020).

[16] Borexino Collaboration, «Identification of the cosmogenic ^{11}C background in large volumes of liquid scintillators with Borexino», arXiv:2106.1097 [cs.CL], submitted for publication to *Eur. Phys. J. C.*

[17] V. Di Marcello *et al.*, «Fluid-dynamics and transport of ^{210}Po in the scintillator Borexino detector: A numerical analysis», *Nucl. Instrum. Methods Phys. Res. A* **964**, 163801 (2020).

The list of Borexino Collaboration members:

M. Agostini, K. Altenmüller, S. Appel, V. Atroshchenko, Z. Bagdasarian, D. Basilico, G. Bellini, J. Benziger, R. Biondi, D. Bravo, B. Caccianiga, F. Calaprice, P. Cavalcante, A. Chepurnov, D. D'Angelo, S. Davini, A. Derbin, A. Di Giacinto, V. Di Marcello, X.F. Ding, A. Di Ludovico, L. Di Noto, I. Drachnev, A. Formozov, D. Franco, C. Galbiati, C. Ghiano, M. Giammarchi, A. Goretti, A.S. Göttel, M. Gromov, D. Guffanti, Aldo Ianni, Andrea Ianni, A. Jany, D. Jeschke, V. Kobychev, G. Korga, S. Kumaran, M. Laubenstein, E. Litvinovich, P. Lombardi, I. Lomskaya, L. Ludhova, G. Lukyanchenko, L. Lukyanchenko, I. Machulin, J. Martyn, E. Meroni, M. Meyer, L. Miramonti, M. Misiaszek, V. Muratova, B. Neumair, M. Nieslony, R. Nugmanov, L. Oberauer, V. Orekhov, F. Ortica, M. Pallavicini, L. Papp, L. Pelicci, O. Penek, L. Pietrofaccia, N. Pilipenko, A. Pocar, G. Raikov, M.T. Ranalli, G. Ranucci, A. Razeto, A. Re, M. Redchuk, A. Romani, N. Rossi, S. Schönert, D. Semenov, G. Settanta, M. Skorokhvatov, A. Singhal, O. Smirnov, A. Sotnikov, Y. Suvorov, R. Tartaglia, G. Testera, J. Thurn, E. Unzhakov, F. Villante, A. Vishneva, R.B. Vogelaar, F. von Feilitzsch, M. Wojcik, M. Wurm, S. Zavatarelli, K. Zuber, G. Zuzel.